ISSN (Print) 1226-1750
ISSN (Online) 2233-6656
Journal of Magnetics 24(1), 168-173 (2019) https://doi.org/10.4283/JMAG.2019.24.1.168

Magnetic Field Analysis of Notched SPMSM Using Conformal Mapping

Young-Yoon Ko[1], Jun-Young Song[1], Myung-Ki Seo[1], Yong-jae Kim[2], and Sang-Yong Jung[1]*

[1]*Sungkyunkwan University, Republic of Korea*
[2]*Chosun University, Republic of Korea*

(Received 15 July 2018, Received in final form 26 November 2018, Accepted 3 December 2018)

We present an analytical method for applying conformal mapping to the notched geometry of a surface permanent magnet synchronous motor to calculate the cogging torque. First, the complex relative air-gap permeance (CRAP) of the notched air-gap is calculated by multiplying the CRAP of a slotted air-gap with the notch sensitivity coefficient, which is defined by the relation of slot and notch shapes. Secondly, the no-load air-gap flux density (AFD) is derived from the CRAPs of the notched and slotted air-gaps. Finally, the cogging torque of the notched motor is calculated by the no-load AFD and is verified using the 2D finite element analysis (FEA) result. A 4-pole and 12-slot surface permanent magnet synchronous motor with the notch is used herein.

Keywords : analytical method, air-gap permeance, conformal mapping, notched motor

1. Introduction

Accurate field distribution analysis is imperative for electric machines. Generally, the analytical method and finite element method (FEM) are conducted to analyze the field solution. In the initial state, multiple finite element analyses (FEAs) are conducted to check the torque density, cogging torque, and back-EMF. For this, time must be spent on drawing the geometry and setting the conditions in order to obtain FEA results. However, a well-established analytical method may provide a proper field solution without wasting time, even though the geometry of the permanent magnet (PM) motor is changed. The most compelling reason for using the analytical method is that the field solution can be calculated simultaneously, compared to FEM.

A surface permanent magnet synchronous motor (SPMSM) is investigated using analytical methods. The precise no-load field solution, involving the radial and tangential components of the air-gap flux density (AFD) of the internal or external SPMSM with radial or parallel magnetization, is presented in [1]. The slotting effect is defined using the complex relative air-gap permeance (CRAP) obtained from the results of the conformal mappings (CMs) of the slot geometry [2]. It also shows that the no-load analysis can be determined by the CRAP of the slotted motor. An analytical method, with a magnetic-equivalent circuit and CM, was recently applied to an interior permanent magnet synchronous machine, as shown in [3]. However, the application of the conformal transformation to SPMSM for the notch effect has not yet been studied. The notch effect based on FEA has been investigated to analyze the flux distribution in air-gap depending on the notch shapes [4, 5]. The notch shape used to apply the stator for reduction of the cogging torque and torque ripple.

In this paper, we propose the novel computational method to calculate the no-load AFD of a notched motor using conformal transformation of a slotted air-gap and the notch sensitivity coefficient. To begin, a notch sensitivity coefficient equation is established by investigation of the relationship between the slot and notch shape. Then, the CRAP of the notched air-gap is obtained by combining the CRAP of the slotted air-gap with the notch sensitivity coefficient. Finally, the CRAPs of the slotted and notched air-gaps are used to derive the no-load AFD distribution. To check the validity of the proposed method, the no-load AFD (radial and tangential components) and cogging torque are compared with the 2D FEA results.

*Corresponding author: Tel: +82-31-299-2952
Fax: +82-31-299-2918, e-mail: syjung@skku.edu

This paper was presented at the IcAUMS2018, Jeju, Korea, June 3-7, 2018.

2. Slotted Model Analysis

Generally, analysis of the slotted model with CM is based on the no-load field solution of the slotless model. Hence, the no-load AFD of the slotless model was calculated [1]. Following this, the slotted shape was transformed into the slotless shape via CM. The CM result of the slotted and slotless shapes is defined as the CRAP [2]. Finally, the combination of the CM result and no-load field solution of the slotless model led to the no-load field solution in the slotted model.

2.1. Slotless SPMSM model analytical method

The general two-dimensional analytical method for predicting the no-load field distribution in radial and parallel magnetizations is presented in [1]. The radial and tangential components of the no-load flux density in the slotless model become

$$B_{slotless\_r} = \Sigma_{n=1,3,5,...}^{\infty} X \cos\{np(\theta - \omega_r t + \theta_{inital})\} \quad (1)$$

$$B_{slotless\_\theta} = \Sigma_{n=1,3,5,...}^{\infty} Y \cos\{np(\theta - \omega_r t + \theta_{inital})\} \quad (2)$$

where X and Y are the motor parameters, p is the number of pole pairs, ω_r is the mechanical angular velocity, and θ_{inital} is the initial angle of the rotor. The air-gap flux density of the slotless SPMSM consists of two components—radial and tangential—and can be written as [1]:

$$B_{slotless} = B_{slotless\_r} + B_{slotless\_\theta}. \quad (3)$$

2.2. Slotted SPMSM model analytical method

The conformal transformation is a significantly useful method for the analytical solution of a Laplacian field with the boundaries of a complicated model. Furthermore, CM is used to transform the slotted model into the slotless model, for which the field distribution is determined using (1) and (2).

The process of the shape change, from the slotted model to the slotless model, has four conformal transformations and five complex planes: the S, Z, W, T, and K planes, as shown in Fig. 1. T_1 transforms the cylinder shape into a polygonal shape and T_4 is the inverse transformation. The Schwarz–Christoffel transformation, represented by T_2 and T_3, is considered important because it is closely related to the calculation of the CRAP. The geometric shapes of the S- and K-planes represent the slotted model and the slotless model, respectively. All descriptions of the complex planes and equations of the transformations are well-established in [6].

After CM, the AFD distribution of the slotted motor in the S-plane can be written in the following form:

$$B_{slot} = B_{slotless} C_{slot}^{*}. \quad (4)$$

where B_{slot} is the AFD of the slotted air-gap, $B_{slotless}$ is the AFD of the slotless air-gap in the K-plane calculated according to (1) and (2), and C_{slot} is the CRAP calculated in detail in [6]. C_{slot} consists of real and imaginary parts in the form

$$C_{slot} = C_{slot\_a} + jC_{slot\_b} \quad (5)$$

B_{slot} is also a complex number, represented as $B_{slot} = B_{slot\_r} + jB_{slot\_\theta}$, and so, it can be rewritten in the following form [2]:

$$B_{slot\_r} = B_{slotless\_r} C_{slot\_a} + B_{slotless\_\theta} C_{slot\_b} \quad (6)$$

$$B_{slot\_\theta} = B_{slotless\_\theta} C_{slot\_a} + B_{slotless\_r} C_{slot\_b}. \quad (7)$$

3. Notched Model Analysis

The analytical method with conformal transformation is frequently used as it takes a similar run-time while changing motor parameters, including the rotor outer diameter, stator outer diameter, and magnet grade. The run-time of the FEA varies depending on the motor size.

In this study, the conformal mapping was adapted to the analysis of the no-load field distribution in the notched motor. The main theory of the notched model analysis is that the CRAP of the notched air-gap is approximated based on the CRAP of the slotted air-gap with the notch sensitivity coefficient. Analysis of the notched motor begins with the slotless model. Then, the notch coefficient is calculated by the relationship between the notched and slotted shapes. After this, a notch CRAP can be defined. Finally, the proposed analytical method of the notch effect can be validated in comparison to the FEM results.

3.1. Notch sensitivity coefficient equation

For the notched model analysis, the notch sensitivity coefficient associated with the notched shape is first established. In Fig. 1, the notch shape is regarded as the slot shape, exempting the geometrical properties of width

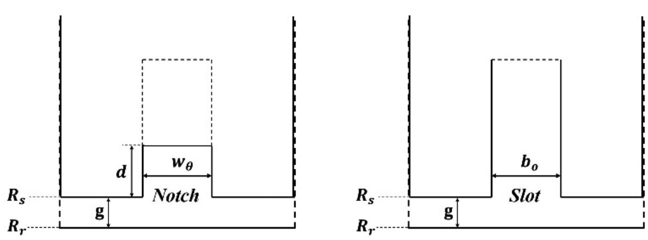

(a) (b)

Fig. 1. Geometric properties of the (a) slot and (b) notch.

Table 1. Notch sensitivity coefficient depending on the depth and width of the notch shape.

d \ w_θ	0.5	1	1.5	2	2.5	3	3.5	4	4.5	5
0.25	1.0158	1.0319	1.0483	1.0649	1.0818	1.0990	1.1164	1.1341	1.1521	1.1704
0.5	1.0149	1.0300	1.0454	1.0610	1.0768	1.0929	1.1092	1.1258	1.1426	1.1596
0.75	1.0139	1.0281	1.0425	1.0571	1.0719	1.0869	1.1021	1.1175	1.1331	1.1489
1.0	1.0130	1.0262	1.0396	1.0532	1.0669	1.0808	1.0949	1.1092	1.1237	1.1384
1.25	1.0121	1.0243	1.0367	1.0493	1.0620	1.0748	1.0879	1.1010	1.1144	1.1279
…						…				
4.25	1.0009	1.0018	1.0027	1.0037	1.0046	1.0055	1.0065	1.0074	1.0083	1.0093
4.5	1	1	1	1	1	1	1	1	1	1

and depth. The only difference is the parameter size between the depths of the notch and slot. Owing to the similarity in the geometry, the notch sensitivity coefficient can be established on the basis of the slot and notch variables, such as depth and width. Generally, the CRAP mainly changes depending on the width; thus, the slot opening b_0 and the notch width w_θ are the critical factors that change the AFD distribution. Therefore, the major CRAP values of the slot and notch models are determined by the width. However, a minor difference of the CRAP between the slotted and notched models occurs depending on the notch depth d. When d is close to 0, the no-load AFD of the notch is higher than that of the slot since the effective air-gap length of the slot shape is longer than that of the notch shape. Meanwhile, when d is close to the slot length, the no-load AFD of the notch is equal to that of the slot. As d increases to a specific length, i.e., one-fifth of the slot length, the no-load AFD gradually decreases; however, beyond this length, the no-load AFD of the notch is equal to that of the slot. The notch sensitivity coefficient, β_{notch}, is defined as

$$\beta_{notch} = \exp\left(1 - \frac{d}{L_{slot}/5}\right)\left(\frac{w_\theta}{360/Q_s}\right) \tag{8}$$

where L_{slot} and Q_s are the slot depth and the number of slots, respectively. β_{notch} is calculated using different values of d and w_θ, as given in Table 1. In this study, L_{slot} is 22.5 mm; thus, the specific length becomes 4.5 mm. Therefore, β_{notch} is 1 if d is 4.5 mm, demonstrating that the notch shape is considered as the slot shape. Additionally, if d is longer than the specific length, β_{notch} is regarded as 1.

3.2. Complex relative air-gap permeance of the notch shape

Figure 2 shows the simplification of the notch and slot geometries and Table 2 lists the design parameters of the notched SPMSM model.

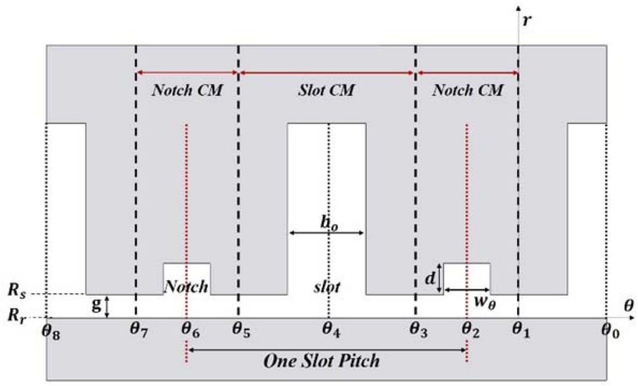

Fig. 2. (Color online) Representation of notch and slot geometries.

Table 2. Design parameters of the slotted and notched SPMSM model.

Parameter	Symbol	Value	Unit
Pole	$2p$	4	-
Slot	Q_s	12	-
Pole-arc/pole-pitch ratio	α_p	0.872	
Air-gap length	g	0.5	mm
Radial thickness of magnet	l_m	2	mm
Stator radius	R_s	40	mm
Magnet radius	R_m	39.5	mm
Rotor radius	R_r	37	mm
Slot opening	b_o	2.8/4°	mm/degree
Stack length	l	50	mm
Magnet remanence	b_r	0.8	T
Relative recoil permeability	μ_r	1.05	-

The CRAP of the notch shape is obtained using the CRAP of a reference and β_{notch}. The CRAP of the reference is the result of conformal transformation, usually used for the slotting effect, based on the notch parameters. It implies that the CRAP of the reference is considered as a slot shape using d and w_θ before post-processing, i.e., before the transformation from slot to notch. The CRAP of the notch shape also comprises real and imaginary components. The real component of the CRAP of the notch shape is expressed as:

$$C_{notch\_a} = C_{slot\_a} \times \beta_{notch} \text{ (within the notch width).} \quad (9)$$

The most crucial point is that C_{slot_a} is the result of CM using notch parameters such as d and w_θ. Further, the imaginary component of the CRAP of the notch shape is defined as

$$C_{notch\_b} = C_{slot\_b} \times (2 - \beta_{notch}). \quad (10)$$

The notch and slot parts exist within one slot pitch, as shown in Fig. 2. Therefore, the new CRAP can be defined as:

Table 3. Notch parameters of the three models.

Parameter	Unit	First model	Second model	Third model
d	mm	0.25	0.5	0.75
w_θ	°	2	3	4
β_{notch}	-	1.0649	1.0929	1.1175

$$C_{new} = \begin{cases} C_{notch}, & (\theta_1 \le \theta < \theta_3) \\ C_{slot}, & (\theta_3 \le \theta < \theta_5) \end{cases}. \quad (11)$$

The wave forms of the real and imaginary parts of C_{new} calculated in the center of the air-gap are shown in Fig. 3. The notch depth and width in Fig. 3 are 0.25 mm and 2°, respectively.

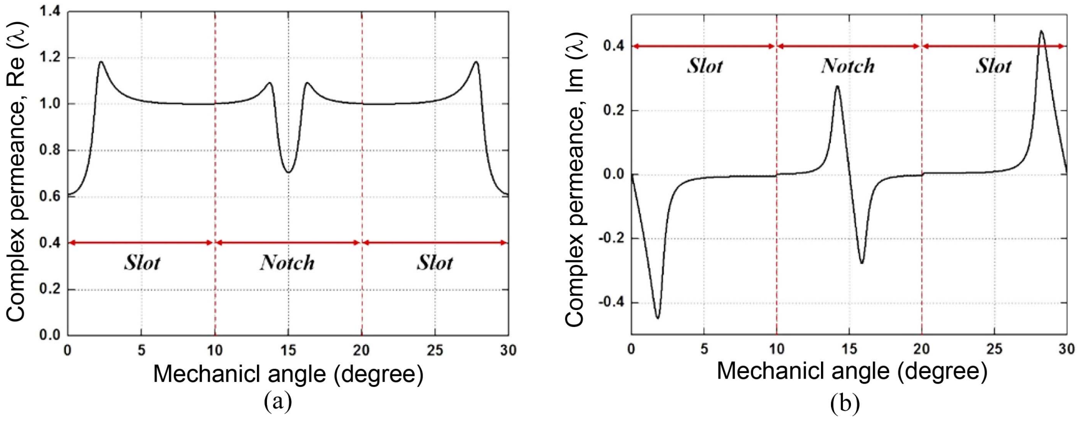

Fig. 3. (Color online) Geometric properties of the (a) slot and (b) notch.

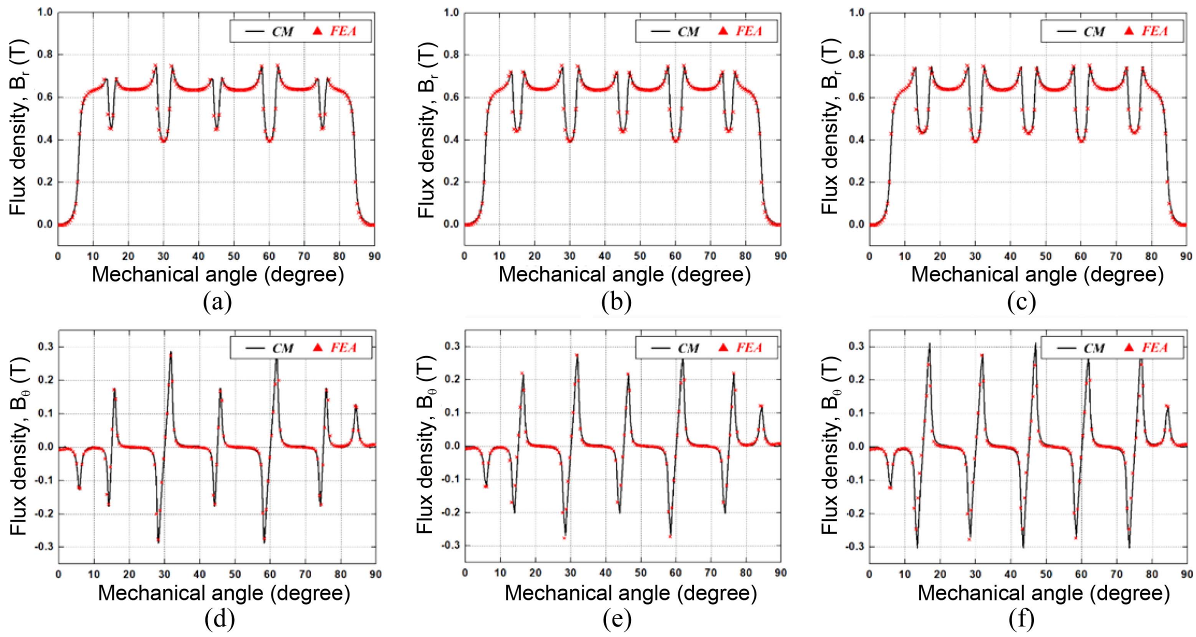

Fig. 4. (Color online) Comparison of flux density waveforms between the proposed analytical method and FEA. B_{new_r} of (a) first model, (b) second model, and (c) third model. B_{new_θ} of (d) first model, (e) second model, and (f) third model.

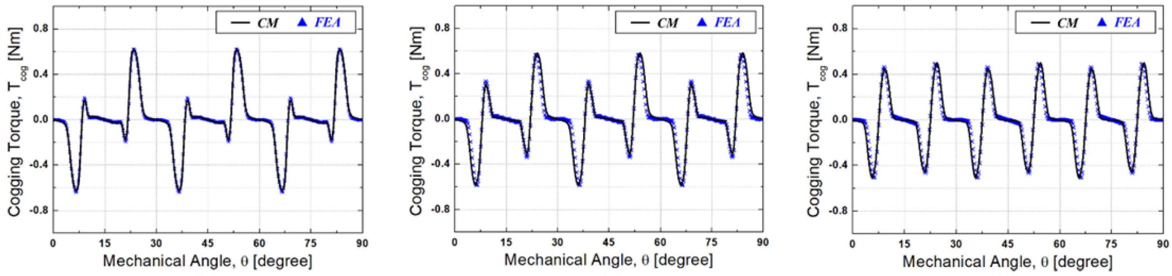

(a) (b) (c)

Fig. 5. (Color online) Comparison of cogging torque waveforms between the proposed analytical method and FEA for (a) first model, (b) second model, and (c) third model.

3.3. No-load air-gap flux density of the notch shape

The no-load AFDs of the slotted and notched air-gaps, B_{new}, can be expressed by

$$B_{new} = B_{new\_r} + B_{new\_\theta} \quad (12)$$

where

$$B_{new\_r} = B_{slotless\_r}C_{new\_a} + B_{slotless\_\theta}C_{new\_b} \quad (13)$$

$$B_{new\_\theta} = B_{slotless\_\theta}C_{new\_a} + B_{slotless\_r}C_{new\_b} \quad (14)$$

$B_{slotless\_r}$ and $B_{slotless\_\theta}$ are the no-load field solutions in the slotless model and are calculated from (1) and (2).

In this study, three notch models are selected, the parameters of which are listed in Table 3.

The three model waveforms of B_{new_r} and B_{new_θ} are shown in Fig. 4. The no-load AFD of the proposed analysis is compared with the FEA result of each model.

The waveforms of the no-load AFD, calculated using the proposed method, agree with the results of the FEA, shown in Fig. 4.

4. Calculation of the Cogging Torque

We calculated the cogging torque of the three models compared to FEA to verify the proposed analytical method. Theoretically, the cogging torque is derived from both the radial and tangential components of the no-load AFD, B_{new_r} and B_{new_θ} of this model. Generally, the cogging torque of the slotted and notched SPMSM models is expressed as

$$T_{cog}(\theta, t) = \frac{l}{\mu_o}r^2\int_0^{2\pi} B_{new\_r}(\theta, t)B_{new\_\theta}(\theta, t)d\theta \quad (15)$$

where B_{new_r} and B_{new_θ} are calculated using (1), (2), (13), and (14); θ denotes the position angle; and t indicates the rotating time. Using the no-load AFD obtained by the proposed method, T_{cog} was also calculated and verified compared to FEA, as shown in Fig. 5.

The waveforms of the proposed method are quite similar to the FEA waveforms. The errors of the obtained cogging torque are within 3 %, indicating that its result is of an acceptable accuracy.

5. Conclusion

This paper introduces the notch effect based on the analytical method of the slotted and notched SPMSM models. The main concept was established by the analysis of the relationship between the slotted shape and the notched shape. As a result, the notch sensitivity coefficient was derived from the notch parameters. Therefore, by transforming the SPMSM model, including the notch into the slotless SPMSM, the CRAPs of the slotted and notched shapes were calculated. Although a change in the notch depth and width led to different forms of the no-load flux density, the analytical calculation of the proposed method yielded reasonable air-gap field solutions. This result was used to calculate the cogging torque. As the flux density was already verified, the cogging torque result was well-matched with the FEA results.

Acknowledgements

This work was supported by "Human Resources Program in Energy Technology" of the Korea Institute of Energy Technology Evaluation and Planning (KETEP), granted financial resource from the Ministry of Trade, Industry & Energy, Republic of Korea. (No. 20184030202190), and National Research Foundation of Korea (NRF) grant funded by the Korea government (MSIT) (NO. 2018R1A2B2006961)

References

[1] Z. Q. Zhu, D. Howe, E. Bolte, and B. Ackermann, IEEE Trans. Magn. **29**, 4414286 (1993).
[2] D. Zarko, D. Ban, and T. A. Lipo, IEEE Trans. Magn. **42**, 8973553 (2006).

[3] D. K Lim, K. P. Yi, D. K. Woo, H. K. Yeo, J. S. Ro, C. G. Lee, and H. K. Jung, IEEE Trans. Magn. **50**, 8201308 (2014).
[4] H. C. Yu, B. S. Yu, J. T. Yu, and C. K. Lin, IEEE Trans. Magn. **50**, 8203104 (2014).
[5] D. Wang, X. Wang, and S. Jung, IEEE Trans. Magn. **48**, 13056459 (2012).
[6] D. Zarko, D. Ban, and T. A. Lipo, IEEE Trans. Magn. **45**, 10729860 (2009).